

Direct Effects of Phosphorylation on the Preferred Backbone Conformation of Peptides: A Nuclear Magnetic Resonance Study

Andreas Tholey,* Almut Lindemann,*# Volker Kinzel,* and Jennifer Reed*

*Department of Pathochemistry, German Cancer Research Center, D-69120 Heidelberg, Germany, and #Lehrstuhl für Biopolymere, Universität Bayreuth, D-95440 Bayreuth, Germany

ABSTRACT Control of protein activity by phosphorylation appears to work principally by inducing conformational change, but the mechanisms so far reported are dependent on the structural context in which phosphorylation occurs. As the activity of many small peptides is also regulated by phosphorylation, we decided to investigate possible direct consequences of this on the preferred backbone conformation. We have performed ^1H nuclear magnetic resonance (NMR) experiments with short model peptides of the pattern Gly-Ser-Xaa-Ser, where Xaa represents Ser, Thr, or Tyr in either phosphorylated or unphosphorylated form and with either free or blocked amino and carboxy termini. The chemical shifts of amide protons and the $^3J_{\text{NH-H}\alpha}$ coupling constants were estimated from one-dimensional and two-dimensional scalar correlated spectroscopy (COSY) spectra at different pH values. The results clearly indicate a direct structural effect of serine and threonine phosphorylation on the preferred backbone dihedrals independent of the presence of charged groups in the surrounding sequence. Tyrosine phosphorylation does not induce such a charge-independent effect. Additionally, experiments with *p*-fluoro- and *p*-nitro-phenylalanine-containing peptides showed that the mere presence of an electronegative group on the aromatic ring of tyrosine does not produce direct structural effects. In the case of serine and threonine phosphorylation a strong dependence of the conformational shift on the protonation level of the phosphoryl group could be observed, showing that phosphorylation induces the strongest effect in its dianionic, i.e., physiological, form. The data reveal a hitherto unknown mechanism that may be added to the repertoire of conformational control of peptides and proteins by phosphorylation.

INTRODUCTION

The control of biological activity in proteins by reversible phosphorylation plays a pivotal role in almost all biochemical processes, from control of catabolism/metabolism through signal transduction to control of growth and gene expression (Marks, 1996). Despite the importance of this posttranslational modification, little is known about exactly how phosphorylation works to alter the activity of a protein (Johnson and Barford, 1993). The physical changes introduced when a hydrogen (of a serine, threonine, or tyrosine side-chain hydroxyl group or at a histidine imidazole) is substituted by a covalently bound phosphoryl group are obvious; steric characteristics, charge, and the ability to form hydrogen bonds are all altered. In some cases, these alone are sufficient to explain the effects observed (Dean and Koshland, 1991; Hurley et al., 1991). The majority of the few mechanisms described so far, however, show phosphorylation works through changing protein conformation in a manner that requires the introduction of the phosphoryl group into an existing network of interactions within the context of a globular protein with well defined tertiary structure (Sprang et al., 1988; Barford and Johnson, 1989, 1992; Barford et al., 1991; Rajagopal et al., 1994).

Cases exist, however, where phosphorylation alters the structural properties of biological peptides with little if any secondary structure and in the absence of a tertiary network, atrial natriuretic peptide (ANP) (Kübler et al., 1992) and the phospholamban peptides (Mortishire-Smith et al., 1995) (Quirk et al., 1996) being prime examples. Where basic residues occur adjacent to the phosphorylation site, the formation of a salt bridge might be the driving factor. Granot et al. (1981), however, found no evidence that this was occurring in phospho Kemptide (L R R A Sp L G) (Kemp et al., 1977) on analyzing the ^{31}P nuclear magnetic resonance (NMR) spectrum, and the crystal structure of glycogen phosphorylase in its phosphorylated form established the absence of a salt bridge to the guanidino groups of the recognition sequence in this case as well (Sprang et al., 1987, 1991). It must also be considered that the formation of salt bridges could not in any case be a universal mechanism as there are biologically active peptides that are phosphorylated by kinases not requiring basic residues as a recognition sequence yet where phosphorylation results in a changed conformation (Larsson et al., 1996; unpublished results).

These observations led to the idea that the presence of a phosphate group might exert direct effects as well as indirect effects on protein conformation, for example, changing the preferred dihedral of the peptide or other adjacent bonds. To look for such direct effects of phosphoryl groups in the absence of tertiary interactions we performed NMR experiments with short synthetic peptides containing serine, threonine, or tyrosine in either the unphosphorylated or the phosphorylated form. Whereas circular dichroism (CD)

Received for publication 11 May 1998 and in final form 20 September 1998.

Address reprint requests to Dr. Andreas Tholey, Department of Pathochemistry, German Cancer Research Center, Im Neuenheimer Feld 280, D-69120 Heidelberg, Germany. Tel.: 49-6221-423257; Fax: 49-6221-423259; E-mail: a.tholey@dkfz-heidelberg.de.

© 1999 by the Biophysical Society

0006-3495/99/01/76/12 \$2.00

spectroscopy allows one to follow the overall conformational changes of peptides after phosphorylation, NMR spectroscopy allows estimation of the ϕ -dihedral in the peptide backbone by measuring the $^3J_{\text{NH-H}\alpha}$ coupling constants. Thus, comparison of the coupling constants of both unphosphorylated and phosphorylated model peptides would allow us to observe possible differences in the preferred populations of backbone conformation. Furthermore, the use of synthetic peptides with artificial sequences permitted the design of peptides with no or only minimal steric hindering and with or without charged groups to study possible direct effects of phosphorylation.

We thus chose the sequence Gly-Ser-Xaa-Ser for our investigations where Xaa represents Ser/Ser(p), Thr/Thr(p), or Tyr/Tyr(p) with either free or blocked amino and carboxy termini to study the influence of charged groups as well. Additionally, we synthesized two peptides with para-fluorinated or para-nitrated phenylalanine instead of tyrosine phosphate (Fig. 1; Table 1) to estimate the effects of other electronegative but uncharged groups on the preferred backbone conformation.

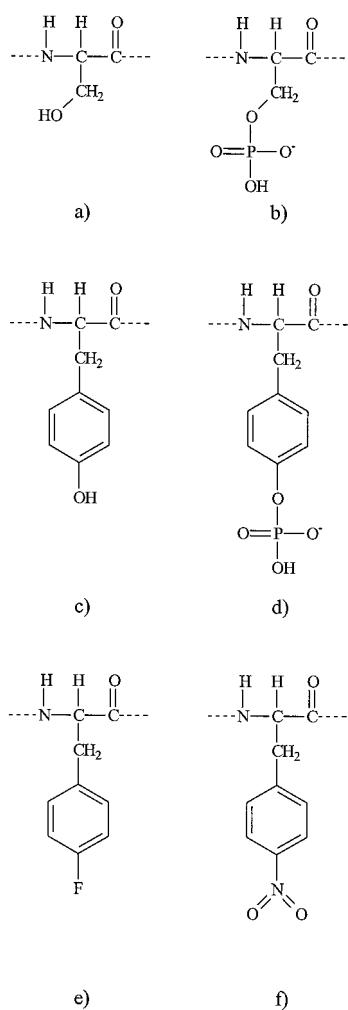


FIGURE 1 Structures of serine (a), phosphoserine (b), tyrosine (c), phosphotyrosine (d), *p*-fluoro-phenylalanine (e), and *p*-nitro-phenylalanine (f) derivatives investigated in this study.

TABLE 1 Peptides investigated in this study

Peptide	Sequence
S	G S S S
Sp	G S Sp S
T	G S T S
Tp	G S Tp S
Y	G S Y S
Yp	G S Yp S
Yf	G S F(<i>p</i> Fluoro) S
Yno ₂	G S F (<i>p</i> Nitro) S
ASN	Ac-G S S S-NH ₂
ASpN	Ac-G S Sp S-NH ₂
ATN	Ac-G S T S-NH ₂
ATpN	Ac-G S Tp S-NH ₂
AYN	Ac-G S Y S-NH ₂
AYpN	Ac-G S Yp S-NH ₂

One- and two-dimensional (1- and 2D) NMR experiments were performed to assign all atoms. The $^3J_{\text{NH-H}\alpha}$ coupling constants were estimated both from 1D and 2D COSY spectra. Additionally, pH titrations were performed to estimate the influence of the ionization state of the phosphate moiety. Both the $^3J_{\text{NH-H}\alpha}$ coupling constants and the chemical shifts of the amide protons were used to investigate potential effects of phosphorylation of hydroxy amino acids on the population of preferred backbone conformations.

Using these techniques, we have been able to establish that the presence of a phosphoryl group covalently attached to certain amino acid side chains can in fact exert a direct effect on the preferred backbone dihedral. To the best of our knowledge, this adds a hitherto unknown mechanism to the repertoire of conformational control of proteins and peptides by phosphorylation.

EXPERIMENTAL PROCEDURES

Peptide synthesis

The peptides were synthesized by standard Fmoc methodology (Fields and Noble, 1990) on an Applied Biosystems ABI 433 automated synthesizer (Applied Biosystems, Weiterstadt, Germany) employing HBTU (*O*-benzotriazol-*N,N,N',N'*-tetramethyluronium hexafluorophosphate) activation. For peptide acids synthesis, preloaded Fmoc-Ser(OtBu)-HMP-resin (*p*-alkoxybenzylalcohol with trityl linker, 0.55 mmol/g; PepChem, Tübingen, Germany) was used; peptide amides were synthesized on Rink amide resin (PepChem). Serine, threonine, and tyrosine were introduced as *tert*-butyl protected derivatives. Fmoc-Gly-OH was used for synthesis of amino-terminal unprotected peptides whereas Ac-Gly-OH was used to introduce the amino-terminal acetyl group. Fmoc-Ser(PO(OH)(OBzl))-OH (Wakamiya et al., 1994), Fmoc-Thr(PO(OH)(OBzl))-OH, and Fmoc-Tyr(PO(OH)₂)-OH were used as building blocks for phosphopeptide synthesis. Fmoc-Phe(*p*-fluoro)-OH, Fmoc-Phe(*p*-nitro)-OH and all other amino acids were purchased from Nova Biochem (Bad Soden, Germany). Cleavage of the peptides was performed with trifluoroacetic acid (TFA)/triisopropylsilane/water (90:8:2, v:v:v) for 2 h at room temperature. Peptides were purified by preparative reversed phase high-pressure liquid chromatography (HPLC; Kromasil, C₁₈, 5 μm , 100 Å) and analyzed by reversed phase HPLC, matrix assisted laser desorption ionization mass spectroscopy (MALDI MS), and electrospray MS (ES-MS). Before the NMR measurements, peptides were lyophilized from water for several times.

NMR spectroscopy

Samples were dissolved in 10 mM phosphate buffer (pH 6.0) to give a concentration of ~5–15 mM (450 μ l) and centrifuged. Afterwards, 50 μ l of D₂O was added. The pH was varied by titration with 0.1 N HCl or 0.1 N NaOH and measured before the addition of D₂O by a combined glass electrode. The pH values measured during pH titration were uncorrected for isotope effects.

All NMR experiments were carried out on Bruker AMX 400 or AMX 600 spectrometers at 283 K. The homonuclear double quantum filtered COSY (Rance et al., 1983), clean total correlation spectroscopy (TOCSY) (Braunschweiler and Ernst, 1983; Griesinger et al., 1988), and rotating frame nuclear Overhauser enhancement spectroscopy (ROESY) (Bax and Davis, 1985) experiments were performed following standard procedures. ROESY experiments were recorded with mixing times of 300 ms. TOCSY experiments were recorded with mixing times of 70 or 80 ms, respectively. In 1D experiments 32,000 data points were collected and 4000 \times 512 data points were collected in TOCSY and ROESY experiments.

The sweep width varied between 8 and 10 ppm for the different peptides. Application of zero filling in the time domain resulted in a data size of 8000 \times 1000 data points in the frequency domain. A sinebell-squared filter with a phase shift of $\pi/4$ before Fourier transformation was used for TOCSY and ROESY. The H₂O resonance was presaturated by continuous irradiation at the resonance frequency during the relaxation delay. All spectra were acquired in the phase-sensitive mode with quadrature detection in all dimensions using the time-proportional phase incrementation technique (Marion and Wüthrich, 1983). Baseline correction was performed for all 2D spectra along the F2 dimension. In addition to the standard Bruker spectrometer control software, the NDee software package (Software Symbiose, Bayreuth, Germany) was used for data processing on X-window workstations. Chemical shift values are reported relative to 2,2-dimethyl-2-silapentane-5-sulfonate.

Estimation of the coupling constants

Spectra for the estimation of coupling constants were measured at pH 4.7 to minimize exchange of amide protons. Coupling constants were extracted from 1D spectra if there was no spectral overlap of amide proton signals. In these experiments, 32,000 data points were collected. Otherwise, double quantum filtered COSY was used for estimation of coupling constants. Either 4000 or 8000 data points in F2 and 512 data experiments in F1 were collected. All data sets were zero-filled once in t_2 . The data were processed without window function and the spin-spin coupling constants $^3J_{\text{NH}\alpha}$ were extracted from the antiphase splitting in COSY cross sections parallel of F2. Distortions arising from the finite line widths were corrected with standard procedures by fitting the NH-C α H cross-peaks with a Lorentzian function (Neuhaus et al., 1985; Redfield and Dobson, 1990). The accuracy of the showed coupling constants is limited by the digital resolution (Hz per point). The error of differences between two measured values (see Table 3) was calculated as $f = \sqrt{f_1^2 + f_2^2}$, with f as the error of the difference and f_1 and f_2 as errors of the measurements. The degree of the experimental error by estimating the coupling constants from 2D spectra is caused by the restriction of the available data space at data point collection.

RESULTS

Standardization of samples

To show that the peptides do not form aggregates at the relatively high concentrations used for the NMR measurements, spectra were recorded with sample concentrations from 5 to 32 mM. No spectral differences were observed in this range of concentrations. A temperature of 283 K was chosen for the measurements to decrease exchange of labile protons and because of better resolution of signals com-

pared with higher temperatures. Due to spectral overlap of amide protons in some of the peptides investigated we performed 2D NMR experiments both to assign the resonances and to resolve the peaks for estimation of coupling constants from COSY spectra. By measuring COSY, TOCSY, and ROESY spectra, we were able to assign all protons; an exception were the Gly1 amide protons in the unprotected peptides because of their rapid exchange with solvent. The 1D and 2D spectra were measured at pH 4.7 to minimize exchange of the labile protons. Chemical shift values were estimated from 2D spectra (Table 2). The $^3J_{\text{NH}\alpha}$ coupling constants were estimated from the 1D spectra for the unprotected peptides and pH titrations and from 1D and 2D COSY spectra for the protected peptides ASN/ASpN, ATN/ATpN, and AYN/AYpN (Table 2). The behavior of α and β protons was not investigated here but was published for the model peptide Gly-Gly-Xaa-Ala earlier (Hoffmann et al., 1994).

Serine phosphorylation

No spectral overlap of amide protons was observed for either the unphosphorylated or the phosphorylated serine peptides GSSS and GSSpS (Fig. 2). After phosphorylation a slight upfield shift of the carboxyl-terminal Ser4-amide proton was observed. The amide proton of the phosphorylated Ser3 shifted 0.28 ppm downfield, whereas the Ser2 amide proton was shifted only slightly downfield (Table 2). Amide protons of Gly1 were exchanged for both peptides. The $^3J_{\text{NH}\alpha}$ coupling constants of the unprotected serine peptides were estimated from 1D spectra, revealing only minor differences after phosphorylation for Ser2 and Ser4. The coupling constant of the phosphorylated residue Ser(p)3, on the other hand, showed a difference of 0.40 ± 0.17 Hz in comparison with the the unphosphorylated residue Ser3 (Table 3). Similar results were found for the unprotected tetrapeptide GGSA/GGSpA (data not shown).

The 1D spectra of the amino- and carboxyl-terminal protected peptide (ASN) showed no overlapping amide resonances whereas in ASpN the Gly1 and Ser4 amide overlapped. The resonance of the phosphorylated residue Ser3 was shifted 0.29 ppm downfield; the other residues were unchanged. The $^3J_{\text{NH}\alpha}$ coupling constants were estimated from both 1D and 2D spectra. The Ser4 coupling constant remained essentially unaffected; Ser2 was affected slightly, but the phosphorylated residue Ser3/Ser(p)3 showed a difference of 0.51 ± 0.16 Hz (1D) or 0.35 ± 0.57 Hz (2D) (Table 3). As may be seen from Table 2, the values of coupling constants estimated from 1D and 2D spectra were very similar.

On pH titration of the protected peptide (ASN) chemical shifts remained the same over the whole pH range. Similar observations were made for the phosphorylated peptide ASpN with the exception of the Gly1-NH and Ser(p)3-NH resonances, which shifted downfield with increasing pH (Table 4). The coupling constants during pH titration were

TABLE 2 Chemical shifts and coupling constants at pH 4.7

Peptide/proton	Chemical shift [ppm]	$^3J_{\text{NH-H}\alpha}$ (Hz), 1D	$^3J_{\text{NH-H}\alpha}$ (Hz), 2D
GSSS			
Ser2-NH	8.80	6.50 ± 0.12	–
Ser3-NH	8.63	7.40 ± 0.12	–
Ser4-NH	8.12	7.20 ± 0.12	–
GSSSpS			
Ser2-NH	8.85	6.60 ± 0.12	–
Ser(p)3-NH	8.91	7.00 ± 0.12	–
Ser4-NH	8.02	7.20 ± 0.12	–
ASN			
Gly1-NH	8.40	5.60/5.81 ± 0.11	5.86/5.86 ± 0.39
Ser2-NH	8.48	6.72 ± 0.11	6.78 ± 0.39
Ser3-NH	8.59	6.83 ± 0.11	6.88 ± 0.39
Ser4-NH	8.36	7.14 ± 0.11	7.17 ± 0.39
ASpN			
Gly1-NH	8.42	(5.29/5.86) ± 0.11	5.81/5.81 ± 0.42
Ser2-NH	8.50	6.51 ± 0.11	6.66 ± 0.42
Ser(p)3-NH	8.88	6.32 ± 0.11	6.53 ± 0.42
Ser4-NH	8.38	(7.23) ± 0.11	7.10 ± 0.42
GSTS			
Ser2-NH	8.83	6.60 ± 0.12	–
Thr3-NH	8.43	8.37 ± 0.12	–
Ser4-NH	8.10	7.27 ± 0.12	–
GSTpS			
Ser2-NH	8.86	6.73 ± 0.12	–
Thr(p)3-NH	8.64	7.45 ± 0.12	–
Ser4-NH	8.06	7.30 ± 0.12	–
ATN			
Gly1-NH	8.39	(–)	(–)
Ser2-NH	8.49	6.58 ± 0.12	6.67 ± 0.39
Thr3-NH	8.42	(7.76) ± 0.12	7.82 ± 0.39
Ser4-NH	8.32	7.03 ± 0.12	7.05 ± 0.39
ATpN			
Gly1-NH	8.39	(–)	(–)
Ser2-NH	8.47	6.77 ± 0.12	6.93 ± 0.59
Thr(p)3-NH	8.64	7.21 ± 0.12	7.29 ± 0.59
Ser4-NH	8.38	(6.92) ± 0.12	7.03 ± 0.59
GSYS			
Ser2-NH	8.66	6.87 ± 0.12	–
Tyr3-NH	8.44	7.92 ± 0.12	–
Ser4-NH	7.93	7.27 ± 0.12	–
GSYpS			
Ser2-NH	8.60	7.41 ± 0.12	–
Tyr(p)3-NH	8.40	8.37 ± 0.12	–
Ser4-NH	8.03	7.39 ± 0.12	–
GSF(pF)S			
Ser2-NH	8.68	6.69 ± 0.12	–
Phe(pF)3	8.52	7.94 ± 0.12	–
Ser4-NH	7.94	7.33 ± 0.12	–
GSF(pNO₂)S			
Ser2-NH	8.67	(–)	6.77 ± 0.33
Phe(pNO ₂)3-NH	8.67	(–)	8.05 ± 0.33
Ser4-NH	8.03	7.36 ± 0.12	7.39 ± 0.33
AYN			
Gly1-NH	8.34	(–)	5.81/5.81 ± 0.39
Ser2-NH	8.34	(7.00) ± 0.11	7.08 ± 0.39
Tyr3-NH	8.40	7.03 ± 0.11	7.02 ± 0.39
Ser4-NH	8.24	7.31 ± 0.11	7.33 ± 0.39
AYpN			
Gly1-NH	8.39	5.76/5.81 ± 0.11	5.78/5.78 ± 0.37
Ser2-NH	8.35	(7.09) ± 0.11	7.03 ± 0.37
Tyr(p)3-NH	8.46	7.03 ± 0.11	7.04 ± 0.37
Ser4-NH	8.32	(7.48) ± 0.11	7.36 ± 0.37

Values in parentheses show overlapped signals; (–), not estimated or uncertain due to spectral overlap; –, not estimated.

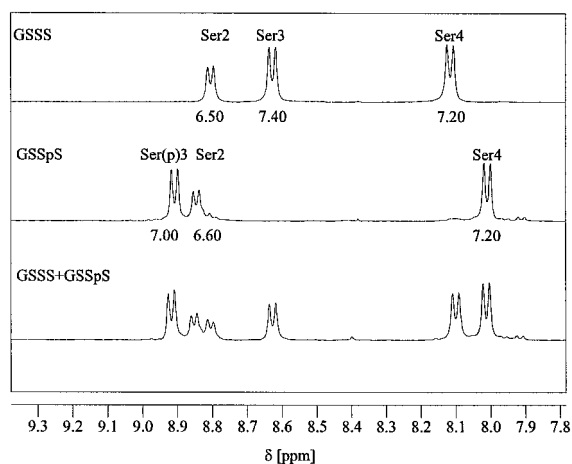


FIGURE 2 One-dimensional spectra of GSSS (top), GSSpS (middle), and a mixture of both (bottom) at pH 4.7 and 283 K. Numbers denote the $^3J_{\text{NH-H}\alpha}$ coupling constants in Hz.

estimated from the 1D spectra only. For the unphosphorylated peptide ASN, the coupling constants remained generally unaffected over most of the pH range but with a slight decrease at higher pH values. For the peptide ASpN a decrease of coupling constants for the phosphorylated serine was observed with increasing pH value. Thus, the difference between the coupling constants of the affected serine in the nonphosphorylated and phosphorylated states increased with increasing pH (Figure 3 a) from $\sim 0.26 \pm 0.16$ Hz at low pH values (below pH 4) to 0.81 ± 0.16 Hz at pH 6.0.

Threonine phosphorylation

With the exception of the exchanged Gly1 amide protons, all amide protons of both the unphosphorylated and the phosphorylated GSTS and GSTpS peptides were well resolved in their 1D spectra. At pH 4.7 the signals of Ser2-NH and Ser4-NH were only slightly altered after phosphorylation, whereas the Thr(p)3 proton shifted downfield (0.28 ppm) (Table 3). The $^3J_{\text{NH-H}\alpha}$ coupling constants of the unprotected serine peptides were estimated from 1D spectra, showing no significant differences for the Ser2 and Ser4 amide protons. Again, however, the coupling constant for the Thr(p)3 amide proton was reduced by 0.92 ± 17 Hz compared with the unphosphorylated residue (Tables 2 and 3).

In the 1D spectra of the amino- and carboxyl-terminal protected peptide (ATN) the resonances of Gly1-NH and Thr3-NH overlapped slightly but still allowed determination of coupling constants (regarding possible error because of this overlap, see below). In the protected phosphorylated peptide ATpN, the amide resonances of Gly1 and Ser4 overlapped, but the other resonances were well resolved. At pH 4.7 signals did not shift significantly after phosphorylation with the exception of Thr3-NH, which shifted downfield for 0.22 ppm in the phosphorylated state (Tables 2 and 3). The $^3J_{\text{NH-H}\alpha}$ coupling constants of both peptides were

estimated from 1D and COSY spectra at pH 4.7. The results of both estimations are very similar (Fig. 4; Tables 2 and 3), showing the applicability and reproducibility of this method even for such slightly overlapped resonances as found in the peptide ATN. The Ser4-NH-H α coupling constant was essentially unaffected by phosphorylation of the adjacent residue; Ser2 showed only a slight effect. The coupling constant of Thr3, however, was reduced by 0.55 ± 0.17 Hz in the 1D spectra after phosphorylation.

On pH titration, the resonances of the unphosphorylated peptide (ATN) were not affected (Figure 5 a). For the phosphorylated peptide (ATpN), a slight downfield shift was observed for the Gly1-NH and Ser4-NH protons, whereas Thr(p)3-NH shifted downfield to a higher extent at higher pH values (Figure 5 b; Table 4). The $^3J_{\text{NH-H}\alpha}$ coupling constants for the peptide ATN were unaffected by changes in pH value under pH 6. Over pH 6, a slight decrease of coupling constant could be observed. For the phosphorylated peptide, coupling constants decreased gradually up to pH 5; at higher pH values a strong decrease was observed. Thus, the difference in the coupling constant of the affected residue between the unphosphorylated and modified peptide increased from $\sim 0.53 \pm 0.16$ Hz at pH 3.5 to 1.14 ± 0.16 Hz at pH 6.4 (Figure 3 b; Table 4).

Tyrosine phosphorylation

At pH 4.7 no spectral overlap was observed for the amide protons of the unprotected peptides GSYS and GSYpS. The Ser4 amide proton was shifted 0.1 ppm to higher field, the Ser2 amide proton was only slightly affected by phosphorylation. Unlike the phosphorylated serine and threonine residues investigated, the phosphorylated tyrosine showed a 0.04 ppm upfield shift in comparison with the unmodified residue (Tables 2 and 3). Substitution of phosphorylated tyrosine by *p*-fluoro-phenylalanine led to minor shifts compared with the peptide GSYS, whereas substitution by *p*-nitro-phenylalanine led to a 0.1 ppm downfield shift of Ser4 but a stronger downfield shift (0.23 ppm) of the amide proton of this residue (Fig. 6; Tables 2 and 3). In the phosphorylated peptide GSYpS the $^3J_{\text{NH-H}\alpha}$ coupling constants of both Ser2 and the phosphorylated residue Tyr(p)3 were increased by 0.54 ± 0.17 Hz and 0.45 ± 0.17 Hz, respectively, whereas the value for Ser4 was only slightly affected. For the *p*-fluoro-Phe-containing peptide only the coupling constant of the Ser2 amide was changed $\sim 0.18 \pm 0.17$ Hz to a lower value. For the *p*-nitro-Phe peptide all coupling constants remained unaffected within limits of error in comparison with the tyrosine peptide GSYS (Tables 2 and 3).

In the protected unphosphorylated peptide (AYN), the resonances of the Gly1 and Ser2 amide protons overlapped slightly, whereas in the phosphorylated derivative the amide signals of Ser2 and Ser4 overlapped. Despite this, determination of coupling constants was possible (see below). The chemical shifts of the phosphorylated peptide (AYpN) dif-

TABLE 3 Chemical shifts and coupling constants at pH 4.7: differences between unphosphorylated and phosphorylated peptides

Peptide/proton	Chemical shift [ppm]	$^3J_{\text{NH-H}\alpha}$ (Hz), 1D	$^3J_{\text{NH-H}\alpha}$ (Hz), 2D
GSSS–GSSpS			
Ser2-NH	−0.05	−0.10 ± 0.17	–
Ser3-/Ser(p)3-NH	−0.28	0.40 ± 0.17	–
Ser4-NH	0.10	0.00 ± 0.17	–
ASN–ASpN			
Gly1-NH	−0.02	(0.31/0.05) ± 0.16	0.05/0.05 ± 0.57
Ser2-NH	−0.02	0.21 ± 0.16	0.12 ± 0.57
Ser3-/Ser(p)3-NH	−0.29	0.51 ± 0.16	0.35 ± 0.57
Ser4-NH	−0.02	−0.09 ± 0.16	0.07 ± 0.57
GSTS–GSTpS			
Ser2-NH	−0.03	−0.13 ± 0.17	–
Thr3-/Thr(p)3-NH	−0.28	0.92 ± 0.17	–
Ser4-NH	0.04	−0.03 ± 0.17	–
ATN–ATpN			
Gly1-NH	0.00	(–)	(–)
Ser2-NH	0.02	−0.19 ± 0.17	−0.26 ± 0.71
Thr3-/Thr(p)3-NH	−0.22	0.55 ± 0.17	0.53 ± 0.71
Ser4-NH	−0.06	0.11 ± 0.17	0.02 ± 0.71
GSYS–GSYpS			
Ser2-NH	0.06	−0.54 ± 0.17	–
Tyr3-/Tyr(p)3-NH	0.04	−0.45 ± 0.17	–
Ser4-NH	−0.10	−0.12 ± 0.17	–
GSYS–GSF(f)S			
Ser2-NH	−0.02	0.18 ± 0.17	–
Tyr3-/Phe(pF)3-NH	−0.08	−0.02 ± 0.17	–
Ser4-NH	−0.01	−0.06 ± 0.17	–
GSYS–GSF(NO ₂)S			
Ser2-NH	−0.01	(–)	−0.10 ± 0.35
Tyr3-/Phe(pNO ₂)3-NH	−0.23	(–)	−0.13 ± 0.35
Ser4-NH	−0.10	−0.09 ± 0.17	−0.12 ± 0.35
AYN–AYpN			
Gly1-NH	−0.05	(–)	0.03/0.03 ± 0.55
Ser2-NH	−0.01	−0.09 ± 0.16	0.05 ± 0.55
Tyr3-/Tyr(p)3-NH	−0.06	−0.07 ± 0.16	−0.02 ± 0.55
Ser4-NH	−0.08	−0.17 ± 0.16	−0.03 ± 0.55

All values were calculated as dephosphopeptide–phosphopeptide. (–), not estimated or uncertain due to spectral overlap; –, value not estimated.

ferred by only small amounts from those of the unphosphorylated peptide (Tables 2 and 3). For the coupling constants also no significant changes at Gly1, Ser2, and Tyr3 were observed; the value for Ser4 differed by a small extent between the two peptides. As before, coupling constants measured from 1D and COSY spectra were very similar, so that determination of coupling constants from 1D spectra was possible despite the slight overlap of the signals.

On pH titration spectral overlap of the protons of the two protected tyrosine peptides occurred, so that we could not measure the coupling constants from 1D spectra over the whole pH range. None of the amide resonances in the unphosphorylated peptide (AYN) shifted over the pH range examined, and the coupling constant of Tyr3-NH was essentially unaffected (Table 4). In the phosphorylated peptide (AYpN), the Gly1-NH shifted to lower field (~0.09 ppm from pH 3.4 to pH 7.1), whereas the other residues remained the same (Table 4). Although the coupling constant of the phosphorylated residue increased slightly at higher pH, this increase cannot be regarded as significant due to the larger error involved in these measurements. The

coupling constants of the other residues could not be read out completely because of spectral overlap or exchange with the solvent but remained unaffected where estimation was possible (Table 4).

DISCUSSION

To look for direct effects of phosphorylation on the preferred backbone conformation we created short peptides containing serine, threonine, and tyrosine in either unphosphorylated or phosphorylated form. We designed these peptides to meet a certain set of requirements. First, neighboring amino acid side chains should not be overly bulky, to prevent steric clashes with the phosphoryl group. Next, to study the influence of charge the peptides should contain no charged groups other than the amino and the carboxy termini. These last are easy to block by acetylation and amidation, respectively, thus allowing the study of charge-based effects without changing the sequence. Finally, peptides were designed to be soluble at high concentrations

TABLE 4 pH titration of amino- and carboxyl-terminal protected peptides

pH	Peptide	Gly1	Ser2	Xaa3/Xaa(p)3	Ser4	SD	Unit
	ASN			Ser3			
3.2		8.40	8.49	8.59	8.36		ppm
		5.49/5.71	6.71	6.78	7.07	±0.11	Hz
4.0		8.40	8.49	8.60	8.36		ppm
		5.68/5.77	6.65	6.79	7.11	±0.11	Hz
4.5		8.40	8.49	8.60	8.36		ppm
		5.08/5.46	6.65	6.74	7.27	±0.11	Hz
5.0		8.40	8.49	8.60	8.36		ppm
		5.43/5.58	6.57	6.79	7.11	±0.11	Hz
5.5		8.40	8.49	8.60	8.36		ppm
		5.43/5.55	6.73	6.79	7.14	±0.11	Hz
6.0		8.40	8.49	8.60	8.36		ppm
		5.68/5.77	6.59	6.65	7.11	±0.11	Hz
6.5		8.40	8.49	8.60	8.36		ppm
		5.40/5.76	(6.23)	(-)	6.93	±0.11	Hz
	ASpN			Ser(p)3			
3.6		8.41	8.49	8.85	8.38		ppm
		5.66/7.39	6.52	6.52	7.47	±0.11	Hz
4.0		8.41	8.50	8.86	8.38		ppm
		(5.74 /?)	6.66	6.48	7.30	±0.11	Hz
4.5		8.41	8.49	8.88	8.38		ppm
		5.77/6.26	6.64	6.42	7.17	±0.11	Hz
5.0		8.43	8.49	8.93	8.38		ppm
		5.60/5.93	6.59	6.32	7.14	±0.11	Hz
5.5		8.51	8.49	9.03	8.38		ppm
		5.99/5.79	6.67	6.18	7.13	±0.11	Hz
6.0		8.50	8.49	9.20	8.38		ppm
		(5.25 /?)	(6.33)	5.84	7.15	±0.11	Hz
6.5		8.53	8.48	9.35	8.36		ppm
		(5.63 /6.43)	6.65	5.48	6.93	±0.11	Hz
	ATN			Thr3			
3.3		8.39	8.49	8.41	8.32		ppm
		5.48/5.75	6.61	7.78	7.03	±0.11	Hz
4.8		8.39	8.49	8.41	8.32		ppm
		5.42/5.63	6.62	7.76	6.95	±0.11	Hz
5.3		8.39	8.49	8.41	8.32		ppm
		5.58/5.58	6.61	7.78	7.04	±0.11	Hz
6.0		8.39	8.49	8.41	8.32		ppm
		5.60/5.63	6.47	7.71	6.96	±0.11	Hz
6.4		8.39	8.49	8.41	8.32		ppm
		5.64/5.33	6.35	7.51	7.04	±0.11	Hz
	ATpN			Thr(p)3			
3.6		8.39	8.46	8.63	8.36		ppm
		5.88/5.14	6.70	7.25	6.73	±0.11	Hz
4.7		8.39	8.46	8.63	8.37		ppm
		(5.92 /3.67)	6.81	7.21	6.92	±0.11	Hz
5.0		8.39	8.46	8.63	8.37		ppm
		(6.14 /3.33)	6.81	7.21	6.97	±0.11	Hz
5.4		8.39–8.41	8.46	8.67	(-)		ppm
		(-)	6.75	7.09	(-)	±0.11	Hz
5.8		8.41	8.46	8.71	8.43		ppm
		(-)	6.75	6.91	(-)	±0.11	Hz
6.4		8.44	8.47	8.83	8.46		ppm
		(-)	6.99	6.37	(-)	±0.11	Hz
6.9		8.51	8.47	9.02	8.56		ppm
		5.41/5.53	6.98	5.41	7.11	±0.11	Hz

Shown are the chemical shifts (ppm, upper values) and the coupling constants ($^3J_{\text{NH-H}\alpha}$ (Hz), lower values) as determined from 1D spectra. Values in parentheses were uncertain or not estimated due to overlap or exchange.

without forming intermolecular aggregates to produce a signal-to-noise ratio in NMR spectroscopy that would allow a proper estimation of coupling constants.

Due to the high resolution conditions of the 1D and 2D spectra, a very accurate estimation of the coupling constants was possible. Those observed are all in a range between 6

TABLE 4 Continued

pH	Peptide	Gly1	Ser2	Xaa3/Xaa(p)3	Ser4	SD	Unit
3.8	AYN	8.35	8.33	Tyr3 8.41	8.24	±0.44	ppm
		(-)	(-)	6.84	7.14		Hz
5.3		8.35	8.33	8.41	8.24	±0.44	ppm
		(-)	(-)	6.81	7.20		Hz
5.8		8.35	8.33	8.41	8.24	±0.44	ppm
		(-)	(-)	6.84	7.18		Hz
6.3		8.35	8.33	8.41	8.24	±0.44	ppm
		(-)	(-)	6.83	7.27		Hz
3.4	AYpN	8.41	8.35	Tyr(p)3 8.45	8.32	±0.44	ppm
		5.45/5.77	7.14	6.89	7.38		Hz
4.9		8.41	8.35	8.45	8.32	±0.44	ppm
		5.47/5.47	7.61	6.88	8.17		Hz
5.5		8.41	8.35	8.45	8.32	±0.44	ppm
		8.45/5.77	6.87	7.00	7.29		Hz
6.0		(-)	8.34	(-)	(-)	±0.44	ppm
		(-)	6.98	(-)	(-)		Hz
6.5		8.47	8.35	8.43	(-)	±0.44	ppm
		5.48/5.90	(6.07)	6.92	(-)		Hz
7.1		8.49	8.35	8.43	(-)	±0.44	ppm
		5.60/5.88	(6.07)	7.25	(-)		Hz

and 7 Hz, which is normal even for peptides with higher populations of ordered structures (Dyson and Wright, 1991). Short peptides are very flexible molecules, and although the amino acids used have a tendency to form nonrandom structures (e.g., turn structures) according to the criteria of Chou and Fasman (1978), it is clearly not to be expected that such peptides will form rigid nonrandom structures in aqueous solutions (Wright et al., 1988). It was therefore not considered worthwhile to attempt to calculate a solution structure or angles from the coupling constants observed, e.g., by the Karplus equation (Karplus, 1959; Pardi et al., 1984). On the other hand, even short peptides have to be regarded as ensembles of dynamic, rapidly interconverting species, thus populating some ordered conformations (Bundi and Wüthrich, 1979; Wright et al., 1988; Dyson and Wright, 1991, 1993; Scholtz and Baldwin, 1992). Therefore, a small difference in coupling constant between unmodified and modified peptides can be a definite indication of a change in the population of the preferred backbone conformation(s).

In the amino- and carboxyl-terminal charged peptides, an alteration in the coupling constants can be seen for the phosphorylated residue after phosphorylation. Additionally, in the case of tyrosine phosphorylation a change can be observed in the coupling constant of the residue amino-terminal to the phosphorylation site. For the protected peptides, changes in the coupling constant for the phosphorylated residue were observed only in the case of the serine and the threonine peptides, whereas the coupling constant in the protected tyrosine peptide was unaffected by phosphorylation. These observations lead to the conclusion that in the case of the charged peptides an additional ionic interaction between the negative phosphoryl group and the positively charged amino terminus or a repulsion from the negatively

charged carboxy terminus was a factor. This effect is stronger in the case of the tyrosine peptide, possibly because of the longer rotational range of the side chain of this amino acid, which allows an interaction with the end groups in the tetrapeptide; in proteins this would mean a possible interaction with charged residues that are at a longer distance from the phosphorylation site. For serine and threonine peptides, on the other hand, although an ionic interaction with the charged end groups may play a partial role, a change in coupling constant is observed after phosphorylation even in the absence of additional charged groups. (For threonine phosphorylation, the effect is slightly stronger than for serine in unprotected peptides, whereas this difference largely disappears with blocking of the termini. This may reflect an additional effect for threonine phosphorylation, where both the side chain methyl group and the phosphoryl group could lead to a steric restriction of the torsion angle χ .) These results show that in the case of serine and threonine peptides, phosphorylation leads to a direct effect on the population of the preferred backbone structure without the necessity of ionic interactions. For tyrosine phosphorylation this effect is absent; no direct structural effects could be deduced where the termini were blocked. A reason for this could be the shielding effect of the aromatic ring, which would attenuate potential interactions between the charged phosphoryl group and the backbone. The experiments with the *p*-fluoro and the *p*-nitro derivatives lead to similar results; these substituents on the phenyl ring are uncharged in contrast to the phosphoryl group, but both remain electronegative groups. In each case no change in the preferred backbone conformation could be observed. Additionally, the amide proton signals of the modified residues are shifted downfield upon phosphorylation in the case of the serine and threonine peptides but not in the case

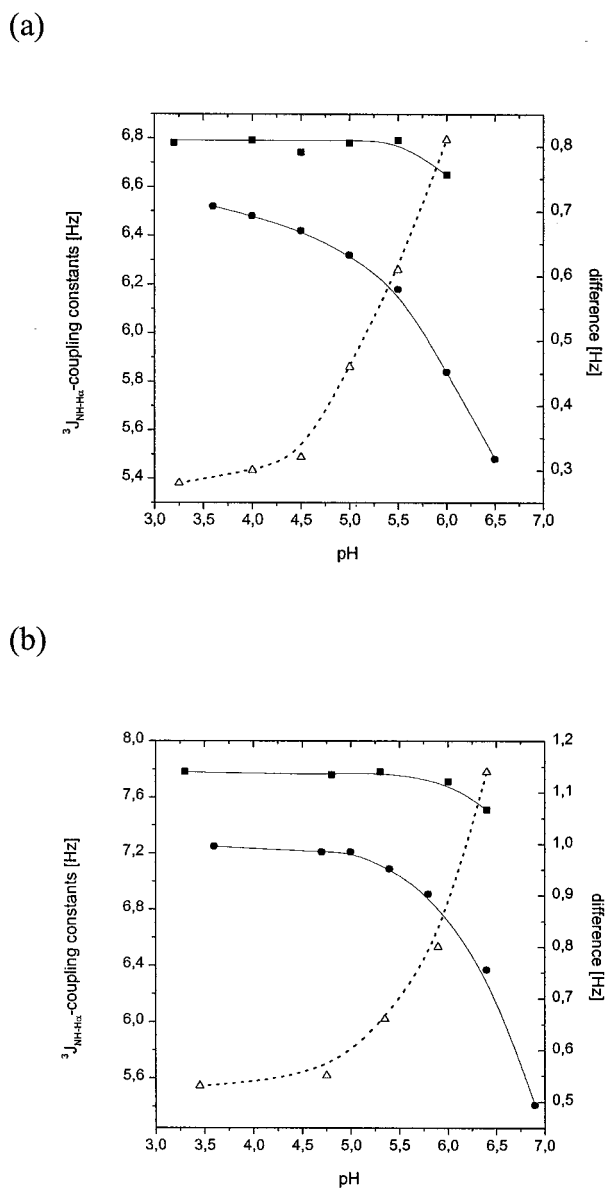


FIGURE 3 Dependence of $^3J_{\text{NH-H}\alpha}$ coupling constants of the modified residue Xaa on pH. (a) Peptides ASN/ASpN; (b) Peptides ATN/ATpN. ■, unphosphorylated residue; ●, phosphorylated residue; - - -, difference between the two values (right scale). The slight decrease shown for the unphosphorylated peptides at higher pH values occurs due to broadening of the signals as fast hydrogen exchange begins.

of the tyrosine peptides. This leads to the conclusion that, in the case of tyrosine phosphorylation, the structural effect observed in unprotected peptides occurs solely due to ionic interactions and, second, that the presence of an electronegative group alone does not alter the structure of the peptide.

Whereas the difference in the coupling constants between phosphorylated and unphosphorylated serine and threonine residues was small but reproducible at pH 4.7, pH titration led to another important observation. The coupling constants decreased for the phosphorylated residue at a much more rapid rate than for the unphosphorylated residue, so that the absolute difference increased at higher pH. The

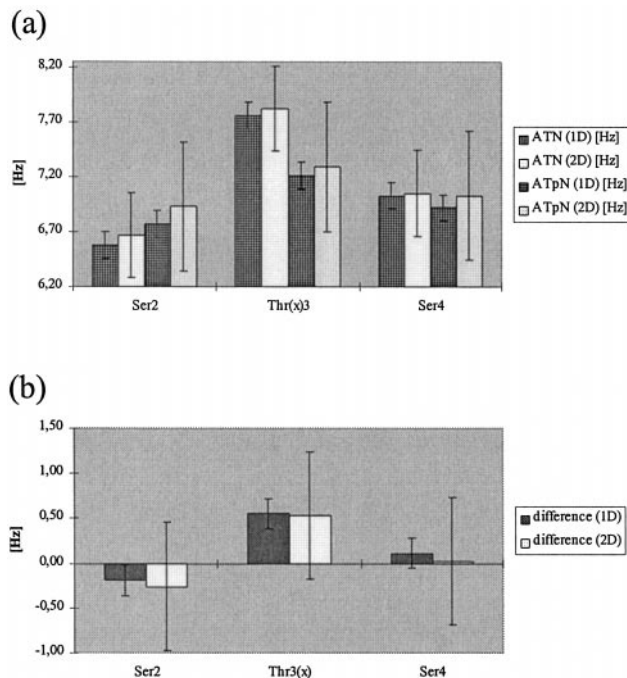


FIGURE 4 Comparison of coupling constants measured from 1D and COSY spectra for peptides ATN/ATpN at pH 4.7 and 283 K. (a) Dark columns, 1D; bright columns, COSY. The first two columns of each block show the unphosphorylated peptides; the next two show the phosphorylated peptides. (b) Difference between the unphosphorylated and the phosphorylated peptide (ATN-ATpN) as estimated from 1D spectra (dark columns) and COSY experiments (bright columns). As noted in the text, the standard error in the COSY data is too high to allow reliable comparison were these taken alone. It can be seen, however, that despite the error level the values obtained correspond closely in absolute value and proportion to the values obtained from 1D spectra.

direct effect of the phosphoryl group on the preferred backbone conformation is thus stronger under physiological conditions, which underscores its potential biological significance. It also means that phosphorylation alters the structure of the peptides most in the dianionic form (the $\text{pK}_{\text{a}1}$ of the phosphoryl group lies below 2, the $\text{pK}_{\text{a}2}$ at 5.9 for phosphoserine and phosphothreonine peptides (Hoffmann et al., 1994)), which may give a clue to the mechanism involved. With respect to this, it is interesting that on pH titration the chemical shifts of the amide protons of the unphosphorylated peptides are either only slightly changed or totally unaffected, whereas the chemical shifts of the phosphorylated residues show an increasing downfield shift with rising pH (Figure 3, a and b). In the tyrosine peptide the phosphorylated residue did not show this pH-dependent downfield shift, reflecting again the shielding effect of the aromatic system.

These observations suggest that H bonds between the amide proton of the phosphorylated residue and the charged phosphoryl group may be the driving force for the direct structural consequences of phosphorylation of serine and threonine residues. Such a mechanism would explain the chemical shift of the affected amide proton, the change in $^3J_{\text{NH-H}\alpha}$ coupling constant of the phosphorylated residue

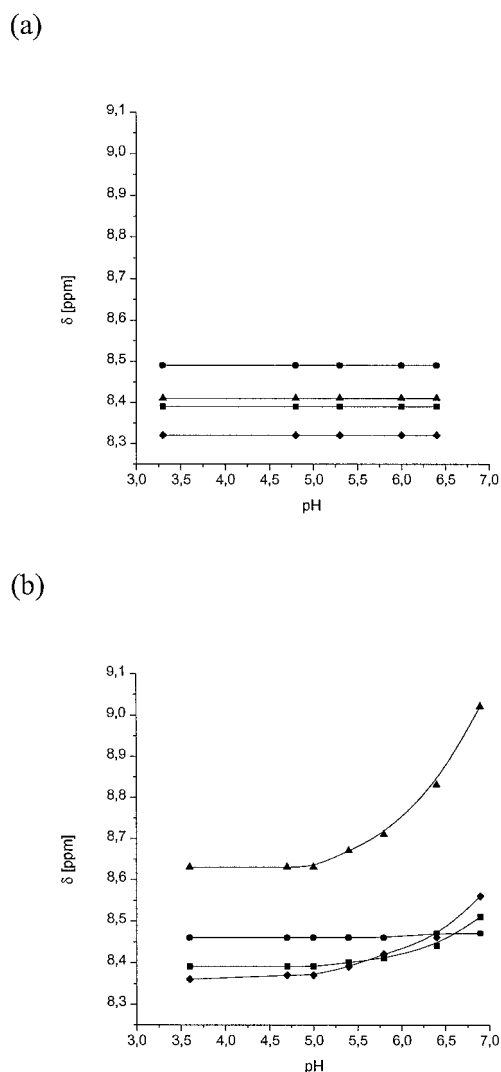


FIGURE 5 Shift of amide protons at pH titration of ATN (a) and ATpN (b). ■, Gly1; ●, Ser2; ▲, Thr3 (a) or Thr(p)3 (b); ◆, Ser4.

indicative of an altered φ angle, and the optimization of the effect of the phosphoryl group when in the dianionic form, i.e., when it can form bifurcated hydrogen bonds with the backbone amide (Figure 7 a). This theory could also explain the behavior of the tyrosine peptides; an intramolecular interaction might be possible only with residues at greater distances, but the amide proton of the phosphorylated residue itself is not properly placed for a stable interaction (Fig. 7, b and c).

Similar results were found earlier in the tetrapeptide Gly-Gly-Glu-Ala (Bundi and Wüthrich, 1979). For this peptide, a small population of ordered structures, for example, β - and γ -bends, was predicted as a consequence of intramolecular H bonds between the negatively charged side chain and backbone amide protons.

The small differences between serine and threonine can be explained by the additional steric restrictions of the threonine side-chain methyl group in combination with the bulky phosphoryl group. Additionally, the more polar phos-

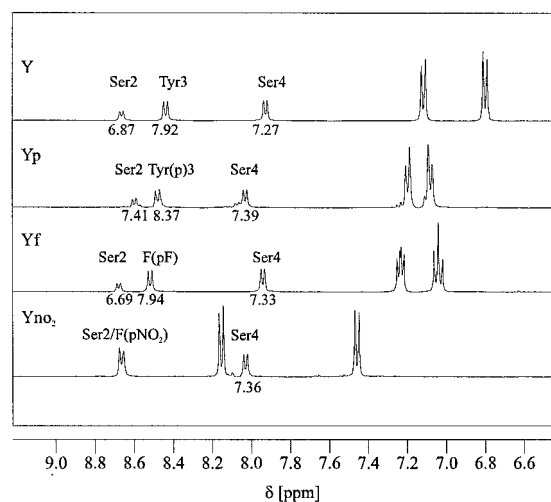


FIGURE 6 One-dimensional spectra of tyrosine peptides and derivatives (from top to bottom: Tyr, Tyr(p), *p*-fluoro-Phe, and *p*-nitro-Phe) at pH 4.7 and 283 K. The resonances not labeled belong to the aromatic protons.

phoryl group will tend to be presented to solvent more frequently than the apolar methyl group, decreasing the probability for interaction with the backbone amides. A direct electronic difference between serine and threonine phosphate appears to be unlikely. The threonine side-chain methyl group exerts an additional electron-pushing effect (+I effect) on the system, which should decrease the effects of an electronegative group such as phosphate. As the effects observed are even stronger for threonine than for serine peptides, a proximity effect of hydrogen/phosphate substitution close to the backbone can be ruled out.

A direct alteration in the preferred backbone dihedral after phosphorylation constitutes a new strategy through which control of biological activity by phosphorylation can be enforced. It would be expected to be of particular importance in small bioactive peptides or in relatively unstructured loops of globular proteins, although it may contribute to the overall effects seen in matrix-dependent systems such as glycogen phosphorylase. It would also play a role in the case of co-translational phosphorylation, where it would assist in predisposing a particular fold on the nascent chain. A provocative aspect is the association of this effect with serine/threonine phosphorylation alone and its absence after tyrosine phosphorylation. Phosphotyrosines play a highly specialized and sequestered role in metabolic control, and they further differ from phosphoserine/threonine residues in having no general consensus sequence for their kinases (Pearson and Kemp, 1991). It is worth considering that the so-called recognition sequences for Ser/Thr kinases may fulfill this role as a secondary function, the presence of adjacent charged residues existing primarily to maximize the effect of side-chain phosphorylation on the backbone dihedral. A fuller understanding of this phenomenon should eventually be useful in the *de novo* design of peptides and proteins.

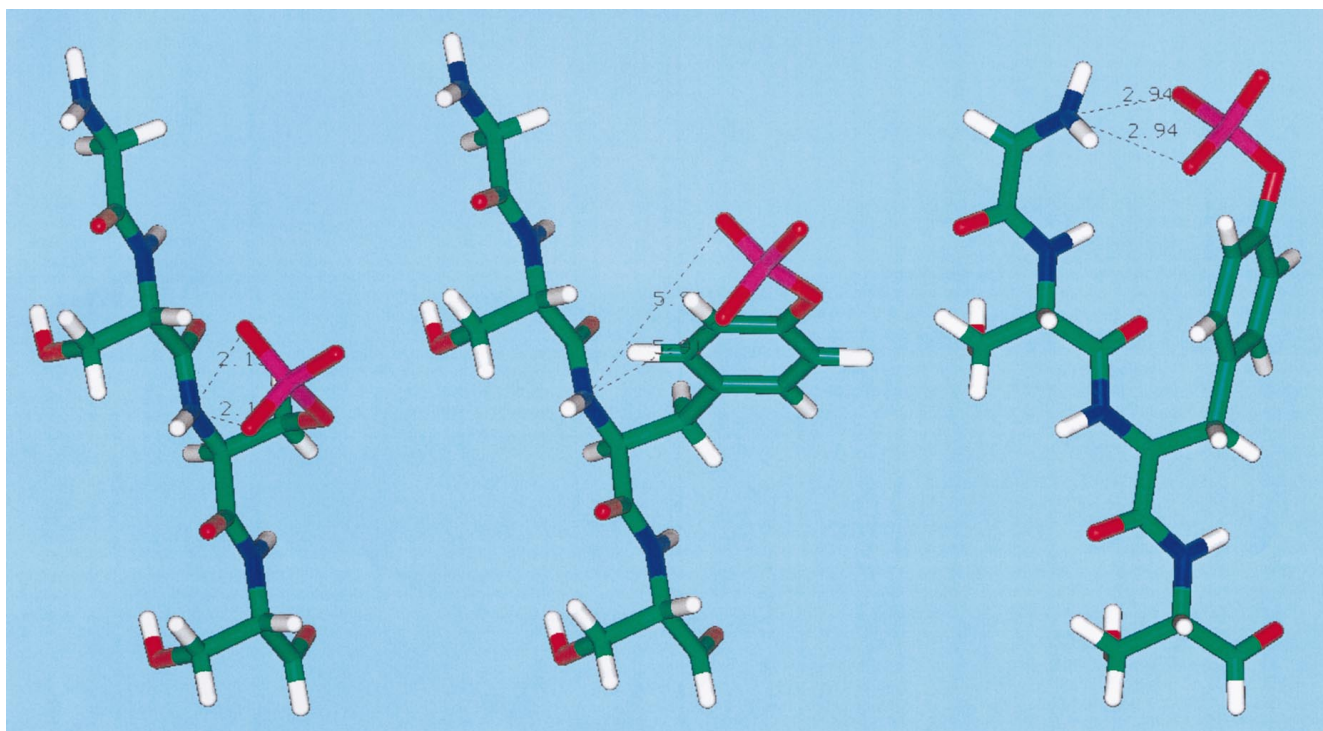


FIGURE 7 Demonstration of the proposed interaction of phosphorylated residues with the peptide backbone amide. The peptide (GSXpS) was held in the extended form and the torsional angles of the phosphorylated side chain altered to ascertain minimal obtainable distance from the potential hydrogen bond donor. The anti-bumping command was used to eliminate van der Waals overlap during the process. (a) Bifurcated H bonding between phosphoryl group on Ser3 and the amide proton of the phosphorylated residue. (b) Minimal distance orientation of the phosphoryl group on a tyrosine residue to the residue's backbone amide. Both the distance and the angle are unfavorable for formation of a hydrogen bond. (c) Minimal distance orientation of phosphoryl group on Tyr3 to the unblocked amino terminus, showing the probable source of the change in coupling constants of the Ser2 and Tyr3 residues in the unprotected peptide. The unprotected amino terminus serves in this case as a model for interactions with distant side chains in oligopeptides and proteins.

We thank Dr. Rüdiger Pipkorn for his assistance with peptide synthesis, Prof. Paul Rösch for helpful discussions, and Mrs. Angelica Lampe for expert preparation of the manuscript.

REFERENCES

- Barford, D., and L. N. Johnson. 1989. Allosteric transition of glycogen phosphorylation. *Nature*. 340:609–616.
- Barford, D., and L. N. Johnson. 1992. The molecular mechanism for the tetrameric association of glycogen phosphorylase promoted by protein phosphorylation. *Protein Sci.* 1:472–493.
- Barford, D., S. H. Hu, and L. N. Johnson. 1991. Structural mechanism for glycogen phosphorylase control by phosphorylation and AMP. *J. Mol. Biol.* 218:233–260.
- Bax, A., and D. G. Davis. 1985. MLEV-17 based two-dimensional homonuclear magnetization transfer spectroscopy. *J. Magn. Reson.* 65:355–360.
- Braunschweiler, L., and R. R. Ernst. 1983. Coherence transfer by isotropic mixing: application to proton correlation spectroscopy. *J. Magn. Reson.* 53:521–528.
- Bundi, A., and K. Wüthrich. 1979. Use of amide ^1H -NMR titration shifts for studies of polypeptide conformation. *Biopolymers*. 18:299–311.
- Chavanieu, A., N. E. Keane, P. G. Quirk, B. A. Levine, B. Calas, L. Wei, and L. Ellis. 1994. Phosphorylation effects on flanking charged residues. *Eur. J. Biochem.* 224:115–123.
- Chou, P. Y., and G. D. Fasman. 1978. Empirical predictions of protein conformation. *Annu. Rev. Biochem.* 47:251–276.
- Dean, A. M., and D. E. Koshland Jr. 1991. Electrostatic and steric contributions to regulation at the active site of isocitrate dehydrogenase. *Science*. 249:1044–1046.
- Dyson, H. J., and P. E. Wright. 1991. Defining solution conformation of small linear peptides. *Annu. Rev. Biophys. Biophys. Chem.* 20:519–538.
- Dyson, H. J., and P. E. Wright. 1993. Peptide conformation and protein folding. *Curr. Opin. Struct. Biol.* 3:60–65.
- Fields, G. B., and R. L. Noble. 1990. Solid phase peptide synthesis utilizing 9-fluorenylmethoxycarbonyl amino acids. *Int. J. Pept. Protein Res.* 35:161–214.
- Granot, J., A. S. Mildvan, H. N. Bramson, N. Thomas, and E. T. Kaiser. 1981. Nuclear magnetic resonance studies of the conformation and kinetics of the peptide-substrate at the active site of bovine heart protein kinase. *Biochemistry*. 20:602–610.
- Griesinger, C., G. Otting, K. Wüthrich, and R. R. Ernst. 1988. Clean TOCSY for ^1H spin system identification in macromolecules. *J. Am. Chem. Soc.* 110:7870–7872.
- Hoffmann, R., I. Reichert, W. O. Wachs, M. Zeppezauer, and H.-R. Kalbitzer. 1994. ^1H and ^{31}P NMR spectroscopy of phosphorylated model peptides. *Int. J. Pept. Protein Res.* 44:193–198.
- Hurley, J. H., A. M. Dean, J. L. Sohl, D. E. Koshland Jr., and R. M. Stroud. 1991. Regulation of an enzyme by phosphorylation at the active site. *Science*. 249:1012–1016.
- Johnson, L. N., and D. Barford. 1993. The effects of phosphorylation on the structure and function of proteins. *Annu. Rev. Biophys. Biomol. Struct.* 22:199–232.
- Karplus, M. 1959. Contact electron spin coupling of nuclear magnetic moments. *J. Phys. Chem.* 30:11–15.
- Kemp, B. E., D. J. Graves, E. Benjamini, and E. G. Krebs. 1977. Role of multiple basic residues in determining the substrate specificity of cyclic AMP-dependent protein kinase. *J. Biol. Chem.* 252:4888–4894.
- Kübler, D., D. Reinhardt, J. Reed, W. Pyerin, and V. Kinzel. 1992. Atrial natriuretic peptide is phosphorylated by intact cells through cAMP-dependent ecto-protein kinase. *Eur. J. Biochem.* 206:179–186.

- Larsson, E., B. Lünig, J. Reed, and C. Krog-Jensen. 1996. Solid phase synthesis of two phosphorylated peptides related to casein using allyl phosphate protection and their CD spectra. *Acta. Chem. Scand.* 50: 1009–1012.
- Marion, D., and K. Wüthrich. 1983. Application of phase sensitive two-dimensional correlated spectroscopy (COSY) for measurements of ^1H - ^1H spin-spin coupling constants in proteins. *Biochem. Biophys. Res. Commun.* 113:967–974.
- Marks, F. (editor). 1996. Protein Phosphorylation. VCH Verlagsgesellschaft, Weinheim, Germany.
- Mortishire-Smith, R. J., S. M. Pitzemberger, C. J. Burke, C. R. Middaugh, V. M. Garsky, and R. G. Johnson. 1995. Solution structure of the cytoplasmic domain of phospholamban. Phosphorylation leads to a local perturbation in secondary structure. *Biochemistry.* 34:7603–7613.
- Neuhaus, D., G. Wagner, M. Vasak, J. H. R. Kägi, and K. Wüthrich. 1985. Systematic application of high resolution, phase-sensitive two-dimensional ^1H -NMR techniques for the identification of the amino-acid-proton spin systems in proteins. *Eur. J. Biochem.* 151:257–273.
- Pardi, A., M. Billeter, and K. Wüthrich. 1984. Calibration of the angular dependences of the amide proton- C^α proton coupling constants, $^3J_{\text{HN}\alpha}$, in a globular protein. *J. Mol. Biol.* 180:741–751.
- Pearson, R. B., and B. E. Kemp. 1991. Protein kinase phosphorylation site sequences and consensus specificity motifs: tabulations. *Methods Enzymol.* 200:63–81.
- Quirk, P. G., V. B. Patchell, J. Colyer, G. A. Drago, and Y. Gao. 1996. Conformational effects of serine phosphorylation in phospholamban peptides. *Eur. J. Biochem.* 236:85–91.
- Rajagopal, P., E. B. Waygood, and R. E. Klevit. 1994. Structural consequences of histidine phosphorylation: NMR characterization of the phosphohistidine form of histidine-containing protein from *Bacillus subtilis* and *Escherichia coli*. *Biochemistry.* 33:15271–15282.
- Rance, M., O. W. Sorensen, G. Bodenhausen, G. Wagner, R. R. Ernst, and K. Wüthrich. 1983. Improved spectral resolution in COSY ^1H -NMR spectra of proteins via double quantum filtering. *Biochem. Biophys. Res Commun.* 117:479–485.
- Redfield, C., and C. M. Dobson. 1990. ^1H NMR studies of human lysozyme: spectral assignment and comparison with hen lysozyme. *Biochemistry.* 29:7201–7214.
- Scholtz, J. M., and R. L. Baldwin. 1992. The mechanism of α -helix formation by peptides. *Annu. Rev. Biophys. Biomol. Struct.* 21:95–118.
- Sprang, S. R., K. R. Acharya, E. J. Goldsmith, D. I. Stuart, K. Varvill, R. J. Fletterick, N. B. Madsen, and L. N. Johnson. 1988. Structural changes in glycogen phosphorylase induced by phosphorylation. *Nature.* 336: 215–221.
- Sprang, S. R., E. Goldsmith, and R. J. Fletterick. 1987. Structure of the nucleotide activation switch in glycogen phosphorylase a. *Science.* 237: 1012–1019.
- Sprang, S. R., S. G. Withers, E. Goldsmith, R. J. Fletterick, and N. B. Madsen. 1991. Structural basis for the activation of glycogen phosphorylase b by adenosine monophosphate. *Science.* 254:1367–1371.
- Wakamiya, T., K. Saruta, J. Yasuoka, and S. Kusumoto. 1994. An efficient procedure for solid phase synthesis of phosphopeptides by the Fmoc-strategy. *Chem. Lett.* 1099–1102.
- Wright, P. E., H. J. Dyson, and R. A. Lerner. 1988. Conformation of peptide fragments of proteins in aqueous solution: implications for initiation of protein folding. *Biochemistry.* 27:7167–7175.